This article is published as part of the *Dalton Transactions* themed issue entitled:

Contributions of Inorganic Chemistry to Energy Research

Guest Editors Duncan Wass and Neil Robertson
University of Bristol and University of Edinburgh, UK

Published in issue 15, 2011 of *Dalton Transactions*

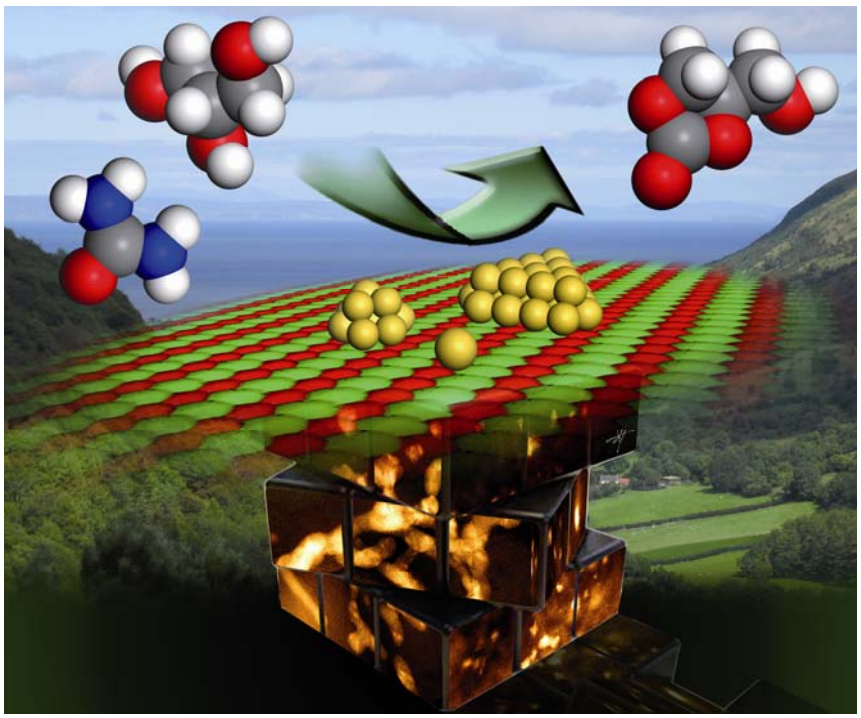

Image reproduced with permission of Graham Hutchings

Articles in the issue include:

ARTICLES:

Visit the *Dalton Transactions* website for more cutting-edge inorganic and organometallic research
www.rsc.org/dalton

Dalton Transactions

Cite this: *Dalton Trans.*, 2011, **40**, 3877

www.rsc.org/dalton

PAPER

Enhancement of photocurrent in dye sensitized solar cells incorporating a cyclometalated ruthenium complex with cuprous iodide as an electrolyte additive†

Hawraa Kisserwan and Tarek H. Ghaddar*

Received 8th November 2010, Accepted 16th December 2010
DOI: 10.1039/c0dt01554g

A new cyclometalated ruthenium complex, [Ru(6′-phenyl-4′-thiophen-2-yl-[2,2′]bipyridinyl-4-carboxylic acid)(4,4′,4″-tricarboxy- 2,2′:6′,2″-terpyridine)]Cl, for Dye Sensitized Solar Cells (DSSCs) is proposed. We have investigated the use of cuprous iodide (CuI) as an electrolyte additive, which in turn has shown photocurrent enhancements of more than 25% in our dye based cells. Using an ionic liquid based electrolyte, an efficiency of $\eta = 5.7\%$ has been accomplished under 1 sun irradiation. The origin of this photocurrent enhancement upon the CuI addition was studied by means of impedance spectroscopy and cyclic voltammetry under dark conditions. The reason behind such a photocurrent enhancement is attributed to an electrocatalytic effect of the CuI on the regeneration of the oxidized dye. Furthermore, the CuI addition did not affect the recombination processes between the injected electrons and the electrolyte nor the electron lifetime in the semiconductor TiO_2 film, which in turn resulted in no changes in the photovoltage.

Introduction

Extensive research has been done in the area of dye sensitized solar cells (DSSC's) since the pioneer work of Grätzel and co-workers on the sensitization of titania, a wide band-gap semiconductor, with a poly-pyridyl ruthenium sensitizer for the fabrication of an efficient and cheap solar cell.[1] Recently, DSSC's efficiencies have reached 11% under AM 1.5 sunlight irradiation, using either the well-known N3 dye (N719 when in the di-anionic form) $[Ru(NCS)_2(dcbpy)_2]$ (dcbpy = 4,4′-dicarboxy-2,2′-bipyridine)[2] or the black dye $[Ru(NCS)_3(tctpy)]$ (tctpy = 4,4′,4″-tricarboxy- 2,2′:6′,2″-terpyridine)[3] as sensitizers. In spite of this, a great deal of research has been performed in the past two decades on the engineering of new ruthenium-based dyes with high molar extinction coefficients in the visible and near-IR in order to out-perform these two dyes. Different strategies have been employed to achieve this goal, such as extending the conjugation in the ancillary ligand,[4–10] modifying the ancillary ligand with electron donating groups,[5,11–16] the use of multi-chromophoric dyes[1,17–19] and recently the introduction of a new class of cyclometalated ruthenium complexes.[20–23] The cyclometalated ruthenium class of dyes is of high importance due to the fact that such complexes lack the thiocyanate ligand (SCN^-), which is considered, from long-term chemical stability tests, as the weakest part in most ruthenium-based dyes.[20,24]

Recently, van Koten *et al.* reported the synthesis and photophysical properties of cyclometalated ruthenium complexes bearing a 2,2′:6′,2″-terpyridine ligand (tpy) and either a substituted 6-phenyl-2,2′-bipyridine (C^N^N′) or a substituted 1,3-dipyridiylbenzene (N^C^N′) as the complementary ligand.[23] In their work it was shown that the ruthenium dyes that possess the (C^N^N′) motifs show better charge injection into TiO_2 than the (N^C^N′) ones. They showed using TD-DFT calculations that the excited state of the former ruthenium complexes is associated with the (C^N^N′) ligand, whereas the latter complexes posses isolated excited states located on the remote tpy ligand. Based on these findings and in continuation of our efforts to engineer new ruthenium-based dyes as strong light absorbers and efficient dyes for DSSC's, we decided to investigate a new cyclometalated ruthenium complex bearing a (tctpy) ligand and a substituted 6-phenyl-2,2′-bipyridyl (C^N^N′) ligand with a thiophene and a carboxylic acid moieties at the 4 and 4′ positions, respectively. The selection of the substituents in this new dye (T66), Scheme 1, were selected for the following reasons: (a) the introduction of a thienyl group would increase the absorption extinction coefficient of the dye in the visible and near-IR region, as shown by many research groups, due to the increase in conjugation, and the large radial extension in bonding when exchanging second row elements by the more electron rich sulfur hetero atom.[11,15,25,26] (b) The four carboxylic acid groups (3 of which are in the deprotonated form) would act as strong anchoring groups to the TiO_2 film, in addition

Department of Chemistry, American University of Beirut, Beirut, 11-0236, Lebanon. E-mail: tarek.ghaddar@aub.edu.lb

† Electronic supplementary information (ESI) available: Cyclic voltammogram (T66) and IPCE of T66 and N719 with EL9 are shown. See DOI: 10.1039/c0dt01554g

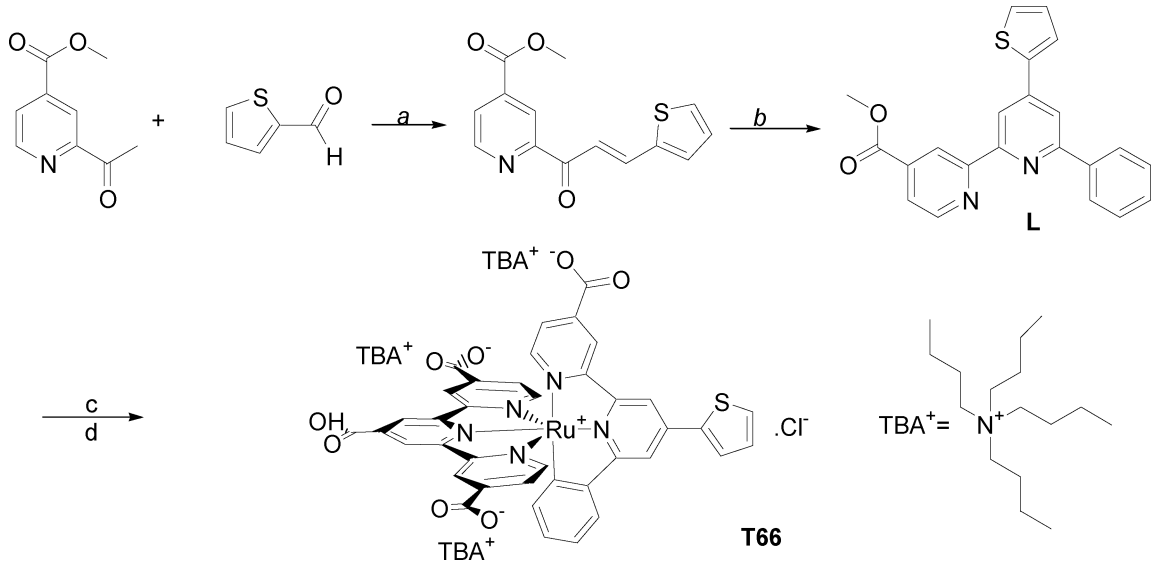

Scheme 1 T66 Synthetic route. (a) pyrrolidinium acetate, methanol, reflux 2 h. (b) ammonium acetate, 1-(2-oxo-phenylethyl)pyridinium iodide, methanol, reflux 4 h. (c) Ru(trimethoxycarbonylterpy)Cl_3, 5 : 2 : 1 ethanol:N-methylmorpholine:H_2O, reflux 24 h. (d) tetra-butylammonium hydroxide, then lowering pH to 3.4 with 0.1 M HCl.

to the neutralization effect of the positive charge present on the ruthenium center.

In the present study, we report the synthesis, electronic, optical, and sensitizing properties of this new cyclometalated dye, T66. The use of cuprous iodide (CuI) as an electrolyte additive and its effect on the T66 performance in a DSSC is also investigated by means of impedance spectroscopy and cyclic voltammetry under dark conditions.

Results and discussion

We were successful in synthesizing the cyclometalated complex T66 by a one-pot reaction protocol between (4,4′,4″-trimethoxycarbonyl-2,2′:6′,2″-terpyridine)$RuCl_3$ and 6′-phenyl-4′-thiophen-2-yl-(2,2′)-bipyridinyl-4-carboxylic acid methyl ester (L), as shown in Scheme 1. The C(H)^N^N′ ligand (L) was synthesized by a multi-step reaction following Krönke[27] methodology starting from 2-thiophenecarboxaldehyde, methyl 2-acetylisonicotinate[28] and 1-(2-oxo-phenylethyl)pyridinium iodide.[29] The complex T66 was characterized by ^{1}H-NMR, APPI-MS, cyclic voltammetry and UV/Vis spectroscopy. The UV/Vis spectra of T66, and N719 as a reference, are shown in Fig. 1. The UV/Vis absorption spectrum of T66 shows in the visible region peaks at 407 nm (ε = 17,800 M^{-1} cm^{-1}) and at 530 nm (ε = 18,600 M^{-1} cm^{-1}) with a shoulder at 650 nm. As can be seen, the absorption extinction coefficient of T66 is higher and the absorption spectrum is shifted more towards the red when compared to N719. The emission spectrum of T66 obtained in air-equilibrated ethanol showed a maximum at 800 nm, Fig. 1.

In order to gain insight into the electronic structure of T66 and to correctly assign the origin of the electronic transitions in the visible region, we performed DFT and TD-DFT calculations on the fully protonated form of T66. The frontier orbitals of T66 are shown in Scheme 2. The HOMO, HOMO-1 and HOMO-2 have a ruthenium t_{2g} character in addition to some contributions from the N^N′^N″ and C^N^N′ ligands. The LUMO, LUMO+2, LUMO+3

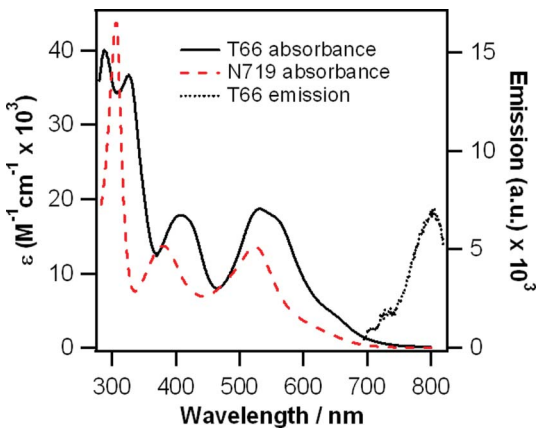

Fig. 1 Absorption (solid-black) and emission (dotted-black) spectra of T66 and absorption spectrum of N719 in ethanol (dashed-red).

and LUMO+4 are π* orbitals delocalized on the N^N′^N″ ligand, whereas the LUMO+1 is a π* orbital delocalized on the C^N^N′ ligand. The predicted absorption spectrum of T66 was performed by TD-DFT calculations using the C-PCM model[30] with water as the solvent. Fig. 2 shows the predicted absorption spectrum of T66 and the experimentally measured one in ethanol. The computed ground-state vertical excitation energies with oscillator strength (*f*) greater that 0.02 are shown in Table 1. As can be seen, the predicted vertical excitations to the red of 400 nm are mainly MLCT transitions with small contributions from intra-ligand LLCT transitions.

The photocurrent *vs.* voltage (IV) response of two cells made with T66 and N719 are shown in Fig. 3. The non-volatile iodide/tri-iodide electrolyte used (EL9, see Table 2) was one which gives a lower voltage but promotes high quantum efficiency of electron injection mainly designed for N719. In this case, T66 shows a lower short circuit current (J_{sc}) of (12.2 mA cm^{-2}) when compared to N719 (15.3 mA cm^{-2}) (Table 2). However, the open

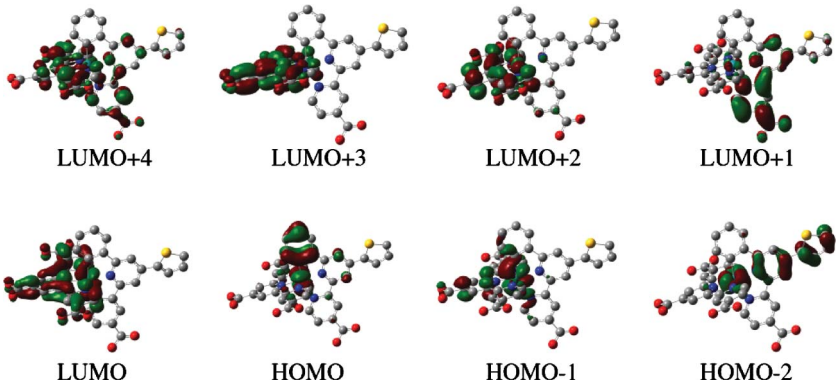

Scheme 2 Frontier Molecular Orbitals of T66.

Table 1 Calculated spectra of T66

TDDFT excitation energies, nm	Oscillator Strength[a]	Assignment
675.8	0.0262	HOMO→LUMO (94%)
576.3	0.0472	HOMO-1→LUMO (59%), HOMO→LUMO+2 (39%)
524.7	0.1044	HOMO-1→LUMO+2 (88%), HOMO-1→LUMO+1 (7%)
502.6	0.2137	HOMO-2→LUMO+1 (34%), HOMO→LUMO+2 (32%), HOMO-2→LUMO+2 (11%)
444.9	0.1744	HOMO→LUMO+3 (94%)
427.6	0.0878	HOMO-1→LUMO+3 (57%), HOMO→LUMO+4 (34%)

[a] Only bands with oscillator strength $f \geq 0.02$ are listed.

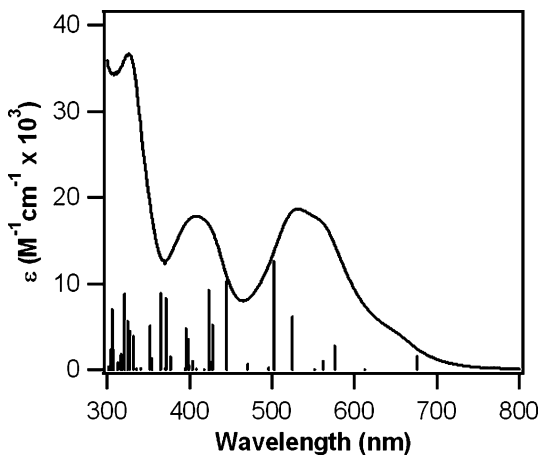

Fig. 2 The computed absorption spectrum of T66 in water (bars) and the measured one in ethanol (solid).

circuit voltage (V_{oc}) of T66 (0.59 V) and that of N719 (0.60 V) were very similar. At first glance, the lower photo-current shown by T66 than N719 was of a surprise, since the UV/Vis absorption spectrum of T66 indicates that it is a stronger light harvester than N719, while assuming that the electron injection efficiencies of T66 and N719 to TiO_2 are similar. Low photo-currents are seen with dyes that have low electron injection efficiencies and/or with dyes that are not efficiently regenerated by the electrolyte. In order to investigate the former case, we calculated the $E_{0\text{-}0}$ = 1.77 eV of T66

Table 2 DSSC Performance of T66 and N719

	Electrolyte[a]	J_{sc}, mA cm^{-2}	V_{oc}, V	*ff*	η %[b]
T66	EL9	12.2	0.59	0.63	4.5
N719	EL9	15.3	0.60	0.67	6.2
T66	EL10	14.7	0.59	0.66	5.7
N719	EL10	15.2	0.59	0.66	5.9

[a] Electrolyte: EL9, methoxypropionitrile (MPN), 0.6 M dimethylpropylimidazolium iodide (DMPII), 0.5 M *tert*-butyl pyridine (TBP) and 0.03 M I_2. EL10, MPN, 0.5 M DMPII, 0.5 M TBP, 0.1 M CuI and 0.03 M I_2. [b] Measured under 100 mW cm^{-2} simulated AM1.5 spectrum with an active area = 0.126 cm^2.

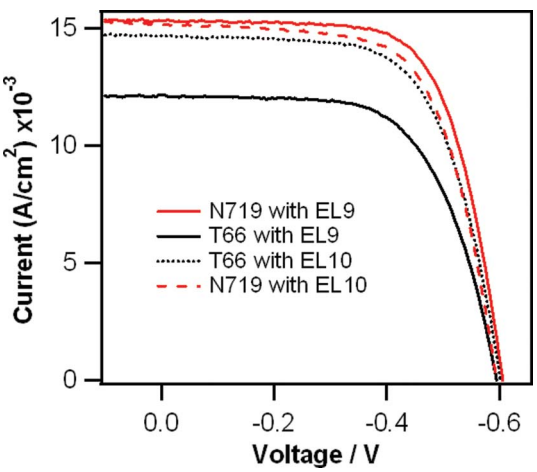

Fig. 3 Photocurrent-voltage (*IV*) curves of: T66/EL9 (solid-black), N719/EL9 (solid-red), T66/EL10 (dotted-black) and N719/EL10 (dashed-red). Measured under 100 mW cm^{-2} simulated AM1.5 spectrum with an active area = 0.126 cm^2.

from the intersection of the normalized absorption and emission spectra of T66. The $Ru^{II/III}$ redox potential of T66 was measured to be $E_{1/2}$ = 0.65 V *vs.* NHE in acetonitrile with $TBAPF_6$ as the supporting electrolyte (Supporting material†). The approximated oxidation potential (E^*_{ox}) of the excited state of T66 is ~ –1.1 V *vs.* NHE, which is more negative than the conduction band level of nanocrystalline TiO_2 (–0.5 V *vs.* NHE).[31] Therefore, upon photo excitation of T66 a fast electron injection into TiO_2 could take place. However, the somehow low $Ru^{II/III}$ redox potential ($E_{1/2}$ = 0.65 V *vs.* NHE) of T66, compared to N719 ($E_{1/2}$ = 1.13 V *vs.* NHE),[2] would suggest that T66 might not be reduced efficiently

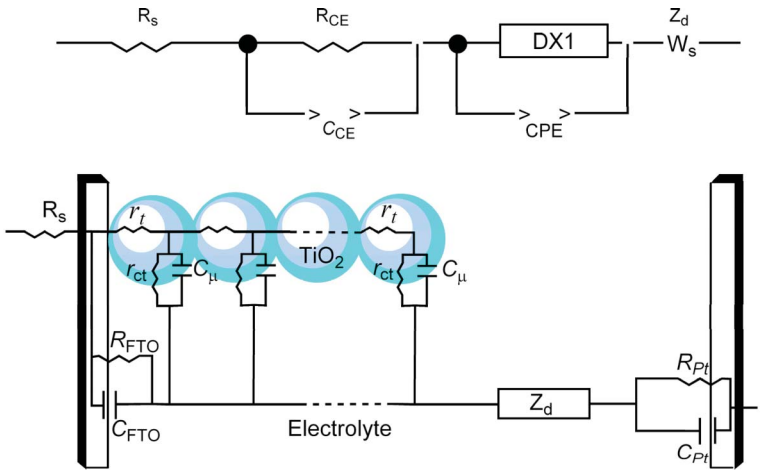

Scheme 3 Equivalent circuit used to fit the impedance measurements and the transmission line model of the DSSC's.

by the iodide electrolyte, since the driving force for such redox reaction in the T66 case is lower by 0.48 V when compared to the N719 case.[32–33]

Cyclometalation affects strongly the redox potentials and photophysical properties of complexes when compared to their non-cyclometalated analogues. The ruthenium(II) oxidation peak shifts to less positive potentials (~ 600 to 800 mV) upon the replacement of a neutral hetero-atom by the anionic carbon center in a multidentate ligand in a ruthenium poly-pyridyl complex.[34] Such cathodic shift in the metal center oxidation potential is due mainly to the increase in the electron density around the ruthenium center upon cyclometalation. As a consequence, the ligand based reduction potentials shift to more negative values due to the increase in back-donation to these ligands. Therefore, this explains the more negative E^{*}_{ox} and the less positive $Ru^{II/III}$ redox potential of T66 when compared to N719.

In 2007 Li-Qan *et al.* reported that the addition of small amount of CuI to an ionic liquid electrolyte increased the photo-current of an N3 based DSSC by 29%.[35] They accounted a part of this increase in the photo-current to an increase in the conductivity of the electrolyte upon the addition of the Cu^{+} cation. In addition, they proposed that the Cu^{+} cation adsorption and/or intercalation into the TiO_2 might be an additional factor in getting higher photo-currents based on the fact that such phenomena can result in a positive shift of the TiO_2 acceptor states, thus better electron injection. Based on this, we decided to investigate the effect of CuI addition to the EL9 electrolyte (designated as EL10) on the T66 DSSC's efficiency. Fig. 3 shows the *IV* curve of a T66 cell with the Cu(I) based electrolyte, EL10. As can be seen, the photo-current increased by ~ 25% to 14.7 mA cm^{-2} and the V_{oc} did not change significantly for T66 compared with the EL9 electrolyte case, while a slight decrease in J_{sc} in the N719 case was detected.

Recently, electrochemical impedance spectroscopy (EIS) has been successfully used for studying electron transport, accumulation, recombination and other interfacial effects in an assembled DSSC.[36–41] We decided to perform EIS on assembled cells in order to understand the reasons behind the significant current increase in T66 cells when the EL10 electrolyte was used. Particularly, we needed to know if the addition of CuI altered the electron transport and/or the electron recombination reactions between the injected electrons and the electrolyte. The impedance spectroscopy was performed in the dark and the applied potential (forward bias) ranged between –0.45 and –0.70 V.[41–43] The transmission line model shown in Scheme 3 was used to describe the system. Under forward bias, electrons are injected from the FTO substrate into the TiO_2 film where the latter is treated as an interconnected network through which electrons propagate with a resistance r_t. Some of the injected electrons can recombine with the oxidized molecules in the electrolyte (I_3^- and/or Cu^{+2} if any are found) with a charge transfer resistance r_{CT} and a capacitance c_{CT}. R_{FTO} and C_{FTO} stand for the charge transfer resistance and double layer capacitance at the FTO/electrolyte interface, where the R_{FTO} would be much larger than r_{CT} under our experimental conditions, *i.e.*; under forward bias of values more negative than –0.45 V the electron recombination takes place mainly from the TiO_2 film to the electrolyte and not at the exposed FTO interface with the electrolyte.[38] The I_3^- diffusion in the electrolyte is described by a Nernst diffusion impedance Z_d, and its reduction to I^- at the platinized counter electrode is characterized by R_{Pt} and C_{Pt}.

Typical EIS of assembled T66 and N719 cells with electrolyte EL9 are shown in Fig. 4 as Nyquist plots. The arc seen in the high frequency region results from the charge transfer resistance and the double layer capacitance at the counter electrode, which is constant at different applied potentials (R_{Pt} and C_{Pt} respectively). However, the arc observed at lower frequencies changes significantly with applied potentials and it is due to the charge transfer resistance (R_{CT}) of the electron recombination and the chemical capacitance at the TiO_2 interface (C_μ). The electrical elements R_{CT}, R_t and C_μ can be extracted by fitting the EIS spectra using an equivalent circuit such as the one shown in Scheme 3. The product of the charge-transfer resistance and the chemical capacitance corresponds to the electron lifetime, $\tau = R_{CT}.C_\mu$. Fig. 5 and 6 show the electron recombination resistance and the electron lifetime in T66 cells, respectively, with EL9 and EL10 electrolytes. As can be seen from the data shown in these two figures, the addition of CuI to the electrolyte did not alter the charge transfer resistance or the electron lifetime in the two different T66 cells. Therefore, one can conclude that the increase in J_{sc} upon the addition of CuI is not due to differences of injection and collection in the two cells. However, the T66 cells made with these two electrolytes do show

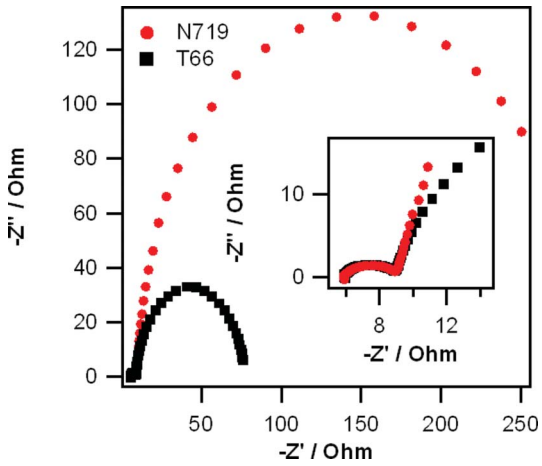

Fig. 4 Impedance spectra of sandwich DSSC with T66/EL9 (black-squares) and N719/EL9 (red-circles) at a potential of –0.6 V. The inset is the high frequency range.

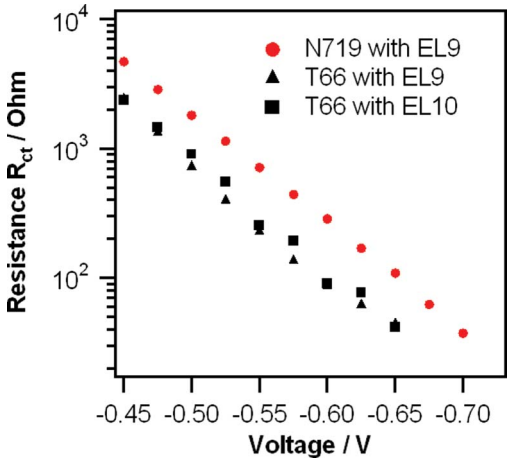

Fig. 5 Charge recombination resistance in N719/EL9 (red-circles), T66/EL9 (black-triangles) and T66/EL10 (black-squares) as a function of applied bias voltage obtained from impedance measurements in the dark.

faster charge recombination processes than in the N719 case. This is not uncommon, since most of the studied dyes in the past two decades show such a phenomenon, and this is what made N719 a paradigm in the DSSC field. These findings led us to investigate closely the second reason (faster regeneration) that might account for the increase in photo-current when using EL10.

We performed cyclic voltammetry with assembled cells of T66 with the two electrolytes under dark and reverse bias conditions, Fig. 7. Under such conditions, as the reverse bias is scanned towards more positive values than 0 V, the anchored dye (either T66 or N719) will get oxidized at a certain voltage and in turn oxidizes the I^- anions in the electrolyte to I_3^-.[44] Therefore, the positive currents seen in the T66 and N719 cells with EL9 are due to the latter redox reaction. Interestingly, the onset (~ 0.3 V) and midpoint (~ 0.6 V) oxidation potential of I^- takes place at the similar values in the T66 and N719 cells with EL9. However, when EL10 is used as the corresponding electrolyte, the onset and midpoint oxidation potential of I^- move towards less positive values by ~ 0.1 V in the T66 case but not for N719. In addition to this, the current density in the EL10 for the above mentioned redox reaction is higher by ~ 25% in both T66 and N719 based cells, and not forgetting that the total ions' concentration is the same in both electrolytes. We speculate that the increase in current density seen with the EL10 based cells is due to an increase in the conductivity of the electrolyte upon the addition of CuI.[35] However, we don't reason the increase in the J_{sc} for the T66 cells with EL10 to the above mentioned increase in conductivity at least in our dye/electrolyte system, which is different from the one studied by Li-Quan *et al.*[35] Another proof that led us to this reasoning is the fact that the use of EL10 with N719 cells did not show any changes in J_{sc} or V_{oc}, yet the current density in the N719/EL10 for the I^- redox reaction is the same as in the T66/EL10 case. In other words, the combined data suggest that both electrolytes' conductivities are not the limiting factors behind the photo-current in our dye/electrolyte system. Alternatively, we think that the N719 dye is getting regenerated efficiently in both electrolytes, while T66 is not regenerated efficiently in EL9, most probably due to the less positive $Ru^{II/III}$ redox potential when

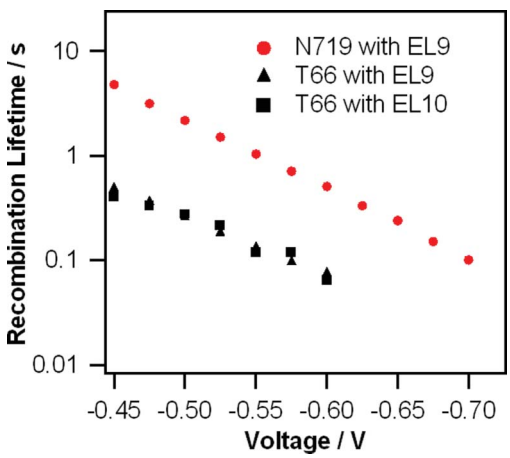

Fig. 6 Electron lifetime in N719/EL9 (red-circles), T66/EL9 (black-triangles) and T66/EL10 (black-squares) as a function of applied bias voltage obtained from impedance measurements in the dark.

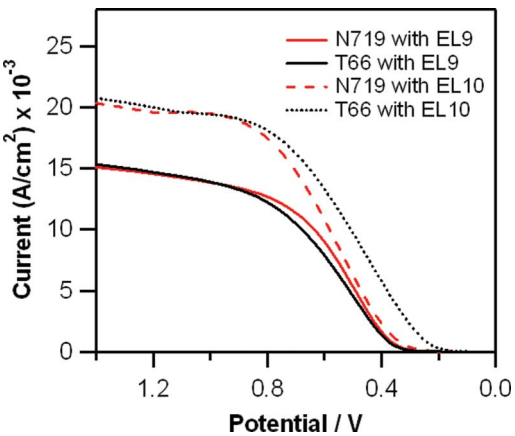

Fig. 7 Cyclic voltammograms of assembled DSSC's of: T66/EL9 (solid-black), N719/EL9 (solid-red), T66/EL10 (dotted-black) and N719/EL10 (dashed-red). Measured in the dark with a sweep rate of 50 mV s^{-1}.

compared to N719. However, upon the addition of CuI (as in electrolyte EL10) the regeneration of T66 is much more efficient than in the EL9 electrolyte. This could explain the 0.1 V shift towards less positive values in the onset and midpoint oxidation potential in the T66/EL10 case. This shift suggests that upon the addition of CuI, the I^- anions are getting oxidized by $T66^+$ at lower potentials than in the T66/EL9 case, not forgetting that T66 gets oxidized at less positive potentials than N719. Therefore, we propose that the CuI is somehow causing an electrocatalytic effect in the T66/EL10 case. In order to eliminate other possibilities for observing such an effect, we performed some control experiments. First, the addition of tetrakis-acetonitrile Cu(I) complex to EL9 showed exactly the same effect as CuI did. Second, the addition of 0.1 M ferrocene to electrolyte EL9 resulted in large deterioration in both the J_{sc} and V_{oc} of the T66 cell. Third, we increased the concentration of I^- up to 1.6 M in EL9 after which the J_{sc} started to decreases, and no positive effect was seen. Lastly, thorough solution cyclic voltammetry of acetonitrile solutions containing TBP, CuI and DMPII individually or combined did not show any *in situ* formed species that have lower redox potentials than T66 or stronger reductants than iodide. Therefore, we speculate that such electrocatalytic effect is taking place at the T66/EL10 interface, where Cu^+ or *in situ* formed Cu(I)-containing species might interact with the T66 monolayer on TiO_2 and cause a more efficient regeneration of the oxidized T66 after electron injection.

Conclusions

We have been successful in synthesizing a new cyclometalated ruthenium complex, T66, and incorporating it as a sensitizer in a DSSC. Efficiencies of 4.5 and 6.2% have been measured for T66 and N719 in a non-volatile ionic liquid based electrolyte, EL9, respectively. However, the addition of CuI to the electrolyte resulted in photocurrent enhancements of more than 25% in the T66 based cells but not for N719. In addition, no changes in photovoltage were seen for T66 and N719 upon the addition of CuI. The origin of this photocurrent enhancement was studied by means of impedance spectroscopy and cyclic voltammetry under dark conditions. The CuI addition did not affect the recombination processes between the injected electrons and the electrolyte nor the electron lifetime in the semiconductor TiO_2 film, which in turn resulted in no changes in the photovoltage. The reason behind such a photocurrent enhancement was attributed to an electrocatalytic effect of the CuI on the regeneration of the oxidized T66 dye.

We are currently investigating this electrocatalytic behavior of CuI in other systems, since such a finding can unveil the possibilities of making new dyes with low $Ru^{II/III}$ redox potential that yet can still work in an iodide/triiodide based DSSC. It is important to mention here that such complexes may have absorption bands shifted to the near-IR due to such higher HOMO's than the classical dyes used in the DSSC research field.

Experimental

Materials and instrumentation

All organic chemicals were purchased from Aldrich and used as supplied. C18- was purchased from YMC (Japan). The N719 dye was purchased from Solaronix (Switzerland). FTO glass "Tec15" was purchased from Pilkington (USA). TiO_2 colloids were purchased from Dyesol (Australia). Ru(trimethoxycarbonylterpy)Cl_3,[45] 1-(2-oxo-phenylethyl)-pyridinium iodide[29] and methyl 2-acetyl isonicotinate[28] were prepared according to reported procedures in the literature. The NMR spectra (^1H and ^{13}C) were measured on a Bruker AM 300 MHz spectrometer. UV-vis spectra were recorded on a Jasco V-570 UV/vis/NIR. Emission spectra were measured on a JobinYvon Horiba Fluorolog-3 spectrofluorometer. The electrochemical setup consisted of a three-electrode cell, with a platinum electrode as the working electrode, a Pt wire ~ 1 mm diameter as the counter electrode, and Ag/Ag^+ (10 mM $AgNO_3$) as the reference electrode. All solution phase electrochemical measurements were done in 0.1 M $TBAPF_6$ in acetonitrile, and Fc/Fc^+ standard (0.63 *vs.* NHE in acetonitrile) was used as a reference. Electrochemical impedance spectra of the DSSC's were performed with a CH instruments 760B (USA). The obtained impedance spectra were fitted with the *Z*-view software (v2.8b, Scribner Associates Inc.). The spectra were performed at various forward bias voltages (from –0.70 to –0.45V) in the frequency range 0.1 Hz–10^5 Hz with oscillation potential amplitudes of 10 mV at RT. The photoanode was connected to the working electrode. The Pt electrode was connected to the auxiliary electrode and the reference electrode. IPCE spectra were recorded using a Newport 74000 Cornerstone™ monochromator and a solar simulator illuminated by a Xenon arc lamp (Oriel) through an AM1.5 simulation filter (ScienceTech). Photocurrent *vs.* Voltage characteristics were measured with a Keithley 2400 sourcemeter. The irradiated area of the cell was 0.126 cm^2.

Computational methods

Calculations were carried out using *Gaussian 03*.[46] Geometries were optimized using the 6-31G* basis set with (B3LYP) together with the Los Alamos effective core potential LanL2DZ[47] in water (C-PCM algorithm).[30] TD-DFT calculations were performed using the C-PCM with water as the solvent. Fifty singlet excited states were determined from the optimized structure of T66. Swizard 2.1 was used for the simulation of the electronic spectrum.[48]

Solar cell fabrication

Dye sensitized solar cells were fabricated using standard procedures. The TiO_2 films were made from colloidal solutions using the doctor blading method and then heated to 480 °C for 30 min. This afforded an 8 μm thick TiO_2 film, on top of which a 4 μm TiO_2 scattering layer (400 nm TiO_2 particles) was deposited and reheated at 480 °C for 30 mins. A $TiCl_4$ post-treatment was applied to the films following reported procedures in the literature.[49] These films were then reheated at 480 °C. Dyeing was done using 0.3 mM solutions in 1 : 1 acetonitrile:*t*-butyl alcohol for N719 and T66. The counter electrodes were fabricated by applying a 2–3 μl cm^{-2} of 5 mM H_2PtCl_6 in 2-propanol to the FTO glass, followed by heating in an oven at 400 °C for 20 min. Cells assemblies were formed by sealing the counter electrodes to the TiO_2 electrode with Surlyn (Dupont) at ~ 100 °C for 1 min. The corresponding electrolyte was introduced through two small holes, previously drilled through the counter electrode, which were then sealed with Surlyn. The electrolytes used were as

follows: EL09, methoxypropionitrile (MPN), 0.6 M 1,3-dimethyl-2-propylimidazolium iodide (DMPII), 0.5 M *tert*-butyl pyridine (TBP), and 0.03 M I_2. EL10, methoxypropionitrile (MPN), 0.5 M DMPII, 0.1 M cuprous iodide (CuI), 0.5 M TBP and 0.03 M I_2.

Preparation of methyl 2-(3-thiophen-2-yl-acryloyl)isonicotinate

To a stirring solution of methyl 2-acetylisonicotinate (3.00 g, 16.80 mmol) and thiophene-2-carbaldehyde (1.80 g, 16.80 mmol) in methanol, pyrrolidinium acetate (2.20 g, 16.80 mmol) was added and the solution was refluxed for 2 h. The precipitate that formed upon cooling was filtered and washed with methanol to yield the desired compound (4.0 g, 87%). ^{1}H-NMR ($CDCl_3$, 300 MHz), δ (ppm): 4.00 (s, 3H), 7.12 (dd, 1H, $J_1 = 3.9$ Hz, $J_2 = 5.1$ Hz), 7.45 (m, 2H), 8.05 (m, 3H), 8.6 (s, 1H), 8.90 (d, 1H, $J = 5.1$ Hz). ^{13}C-NMR ($CDCl_3$, 75 MHz), δ (ppm): 52.9, 119.2, 125.5, 127.3, 128.3, 129.1, 131.5, 134.1, 137.0, 143.1, 152.0, 154.3, 165.9, 187.0. MS (APPI): $m/z = 274.0$ $[M+H^+]^+$ calculated for $C_{14}H_{12}NO_3S$, 274.3.

Preparation of 6′-phenyl-4′-thiophen-2-yl-[2,2′]bipyridinyl-4-carboxylic acid methyl ester (L)

Methyl-2-(3-thiophen-2-yl-acryloyl)isonicotinate (0.30 g, 1.16 mmol) and 1-(2-oxo-phenylethyl)pyridinium iodide (0.39 g, 1.16 mmol) were added to a solution of excess ammonium acetate (2 g) in methanol (20 ml). The resulting solution was then refluxed for 4 h. The precipitate formed upon cooling was collected by filtration. Yield (0.37 g, 85%). ^{1}H-NMR ($CDCl_3$, 300 MHz), δ (ppm): 4.02 (s, 3H), 7.19 (dd, 1H, $J_1 = 4.8$ Hz, $J_2 = 3.9$ Hz), 7.45–7.56 (m, 4H), 7.71 (dd, 1H, $J_1 = 1.2$ Hz, $J_2 = 3.6$ Hz), 7.89 (dd, 1H, $J_1 = 1.5$ Hz, $J_2 = 4.8$ Hz), 7.97 (d, 1H, $J = 1.5$ Hz), 8.20 (m, 2H), 8.63 (d, $J = 1.8$ Hz), 8.86–8.81 (dd, 1H, $J_1 = 0.9$ Hz, $J_2 = 5.1$ Hz), 9.14 (m, 1H). ^{13}C-NMR ($CDCl_3$, 75 MHz), δ (ppm): 52.8, 115.9, 117.2, 120.8, 122.9, 125.7, 127.1, 128.4, 128.8, 129.3, 138.4, 139.1, 141.7, 143.3, 149.8, 155.7, 157.3, 157.6, 165.9. MS (APPI): $m/z = 373.1$ $[M+H^+]^+$ calculated for $C_{22}H_{17}N_2O_2S$, 373.4.

Preparation of [Ru(6′-phenyl-4′-thiophen-2-yl-[2,2′]bipyridinyl-4-carboxylic acid)(4,4′,4″-tricarboxy- 2,2′:6′,2″-terpyridine)]Cl·3TBA, (T66)

The ligand L (0.10 g, 0.27 mmol) and (4,4′,4″-trimethoxycarbonyl-2,2′:6′,2″-terpyridine)$RuCl_3$ (0.16 g, 0.27 mmol) were dissolved in ethanol–H_2O (5 : 1 v/v, 60 ml) followed by the addition of N-methylmorpholine (20 ml). The mixture was then refluxed under Ar for 24 h. The solvent was then evaporated under reduced pressure. The dark solid was then dissolved in water containing excess tetra-butyl ammonium hydroxide and applied to a preparative C18-column. The compound was purified by a gradient elution with water–methanol 100%:0% to 60%:40%. Concentrating the solvent that contains the major violet band under reduced pressure and acidifying it to pH 3.4 with 0.1 M HCl resulted in a dark precipitate. The solid was filtered to yield (0.26 g, 62%) of a dark violet crystalline solid. ^{1}H-NMR (MeOD + 0.1% KOD, 300 MHz), δ (ppm): 0.90–1.05 (t, 36H), 1.39–1.44 (m, 24H), 1.64–1.69 (m, 24H), 3.33 (m, 24H), 5.64 (d, 1H, $J = 7.2$ Hz), 6.51 (t, 1H), 6.77 (t, 1H), 7.39 (dd, 1H, $J_1 = 3.6$ Hz, $J_2 = 4.8$ Hz), 7.52–7.62 (m, 6H), 7.74 (d, 1H, $J = 4.5$ Hz), 7.79 (d, 1H, $J = 7.5$ Hz), 8.14 (d, 1H, $J = 2.7$ Hz), 8.53 (s, 1H), 8.78 (s, 1H), 8.97 (s, 1H), 9.06 (s, 1H), 9.23 (s, 1H). MS (APPI): $m/z = 1548.0$ $[M–Cl^-]^+$ calculated for $C_{87}H_{129}N_8O_8RuS$, 1548.1.

Acknowledgements

This work was supported by the University Research Board (URB) at the American University of Beirut (AUB), the Lebanese National Council for Scientific Research (LNCSR), and the Munib and Angela Masri Institute of Energy.

References

1 B. O'Regan and M. Grätzel, *Nature*, 1991, **353**, 737–740.
2 M. K. Nazeeruddin, F. De Angelis, S. Fantacci, A. Selloni, G. Viscardi, P. Liska, S. Ito, B. Takeru and M. Grätzel, *J. Am. Chem. Soc.*, 2005, **127**, 16835–16847.
3 Y. Chiba, A. Islam, Y. Watanabe, R. Komiya, N. Koide and L. Han, *Jpn. J. Appl. Phys.*, 2006, **45**, L638–L640.
4 A. Abbotto, C. Barolo, L. Bellotto, F. De Angelis, M. Grätzel, N. Manfredi, C. Marinzi, S. Fantacci, J. H. Yum and M. K. Nazeeruddin, *Chem. Commun.*, 2008, 5318–5320.
5 F. Gao, Y. Cheng, Q. Yu, S. Liu, D. Shi, Y. Li and P. Wang, *Inorg. Chem.*, 2009, **48**, 2664–2669.
6 C. Klein, M. K. Nazeeruddin, P. Liska, D. Di Censo, N. Hirata, E. Palomares, J. R. Durrant and M. Grätzel, *Inorg. Chem.*, 2005, **44**, 178–180.
7 P. Wang, C. Klein, R. Humphry-Baker, S. M. Zakeeruddin and M. Grätzel, *J. Am. Chem. Soc.*, 2005, **127**, 808–809.
8 D. Kuang, C. Klein, S. Ito, J. E. Moser, R. H. Baker, N. Evans, F. Duriaux, C. Grätzel, S. M. Zakeeruddin and M. Grätzel, *Adv. Mater.*, 2007, **19**, 1133–1137.
9 M. K. Nazeeruddin, T. Bessho, L. Cevey, S. Ito, C. Klein, F. De Angelis, S. Fantacci, P. Comte, P. Liska, H. Imai and M. Grätzel, *J. Photochem. Photobiol., A*, 2007, **185**, 331–337.
10 K. J. Jiang, N. Masaki, J. B. Xia, S. Noda and S. Yanagida, *Chem. Commun.*, 2006, 2460–2462.
11 F. Matar, T. H. Ghaddar, K. Walley, T. DosSantos, J. R. Durrant and B. O'Regan, *J. Mater. Chem.*, 2008, **18**, 4246–4253.
12 D. Kuang, S. Ito, B. Wenger, C. Klein, J.-E. Moser, R. Humphry-Baker, S. M. Zakeeruddin and M. Grätzel, *J. Am. Chem. Soc.*, 2006, **128**, 4146–4154.
13 C. Y. Chen, M. Wang, J. Y. Li, N. Pootrakulchote, L. Alibabaei, C. H. Ngoc-le, J. D. Decoppet, J.-H. Tsai, C. Grätzel, C.-G. Wu, S. M. Zakeeruddin and M. Grätzel, *ACS Nano*, 2009, **3**, 3103–3109.
14 J. F. Yin, D. Bhattacharya, Y. C. Hsu, C. C. Tsai, K. T. Lu, H. C. Lin, J. G. Chen and K. C. Ho, *J. Mater. Chem.*, 2009, **19**, 7036–7042.
15 H. Kisserwan and T. H. Ghaddar, *Inorg. Chim. Acta*, 2010, **363**, 2409–2415.
16 P. R. F. Barnes, L. Liu, X. Li, A. Y. Anderson, H. Kisserwan, T. H. Ghaddar, J. R. Durrant and B. C. O'Regan, *Nano Lett.*, 2009, **9**, 3532–3538.
17 W. M. Campbell, A. K. Burrell, D. L. Officer and K. W. Jolley, *Coord. Chem. Rev.*, 2004, **248**, 1363–1379.
18 S. R. Jang, R. Vittal, J. Lee, N. Jeong and K. J. Kim, *Chem. Commun.*, 2006, 103–105.
19 A. H. Younes and T. H. Ghaddar, *Inorg. Chem.*, 2008, **47**, 3408–3414.
20 T. Bessho, E. Yoneda, J.-H. Yum, M. Guglielmi, I. Tavernelli, H. Imai, U. Rothlisberger, M. K. Nazeeruddin and M. Grätzel, *J. Am. Chem. Soc.*, 2009, **131**, 5930–5934.
21 S. H. Wadman, J. M. Kroon, K. Bakker, M. Lutz, A. L. Spek, G. P. van Klink and G. van Koten, *Chem. Commun.*, 2007, 1907–1909.
22 T. Funaki, M. Yanagida, N. Onozawa-Komatsuzaki, K. Kasuga, Y. Kawanishi, M. Kurashige, K. Sayama and H. Sugihara, *Inorg. Chem. Commun.*, 2009, **12**, 842–845.
23 S. H. Wadman, J. M. Kroon, K. Bakker, R. W. A. Havenith, G. P. M. van Klink and G. van Koten, *Organometallics*, 2010, **29**, 1569–1579.
24 M. Grätzel, *Acc. Chem. Res.*, 2009, **42**, 1788–1798.
25 J. J. Kim, K. Lim, H. Choi, S. Fan, M. S. Kang, G. Gao, H. S. Kang and J. Ko, *Inorg. Chem.*, 2010, **49**, 8351–8357.
26 M. Wang, S. J. Moon, D. Zhou, F. Le Formal, N. L. Cevey-Ha, R. Humphry-Baker, C. Grätzel, P. Wang, S. M. Zakeeruddin and M. Grätzel, *Adv. Funct. Mater.*, 2010, **20**, 1821–1826.

27 F. Kroehnke, *Synthesis*, 1976, **1**, 1–24.
28 C. Mikel and P. G. Potvin, *Polyhedron*, 2002, **21**, 49–54.
29 J. K. Son, L. X. Zhao, A. Basnet, P. Thapa, R. Karki, Y. Na, Y. Jahng, T. C. Jeong, B. S. Jeong, C. S. Lee and E. S. Lee, *Eur. J. Med. Chem.*, 2008, **43**, 675–682.
30 M. Cossi and V. Barone, *J. Chem. Phys.*, 2001, **115**, 4708–4717.
31 A. Hagfeldt and M. Grätzel, *Chem. Rev.*, 1995, **95**, 49–68.
32 J. Datta, A. Bhattacharya and K. K. Kundu, *Bull. Chem. Soc. Jpn.*, 1988, **61**, 1735–1742.
33 G. Boschloo and A. Hagfeldt, *Acc. Chem. Res.*, 2009, **42**, 1819–1826.
34 S. H. Wadman, M. Lutz, D. M. Tooke, A. L. Spek, F. Hartl, R. W. A. Havenith, G. P. M. van Klink and G. van Koten, *Inorg. Chem.*, 2009, **48**, 887–1900.
35 C. Lie-Hang, X. Bo-Fei, L. Xi-Zhe, L. Ke-Xin, L. Yan-Hong, M. Qing-Bo, W. Rui-Lin and C. Li-Quan, *Chin. Chem. Lett.*, 2007, **24**, 555–558.
36 J. Bisquert and V. S. Vikhrenko, *J. Phys. Chem. B*, 2004, **108**, 2313.
37 K. Zhu, N. Kopidakis, N. R. Neale, J. van de Lagemaat and A. J. Frank, *J. Phys. Chem. B*, 2006, **110**, 25174–25180.
38 F. Fabregat-Santiago, J. Bisquert, G. Garcia-Belmonte, G. Boschloo and A. Hagfeldt, *Sol. Energy Mater. Sol. Cells*, 2005, **87**, 117–131.
39 F. Fabregat-Santiago, J. Bisquert, E. Palomares, L. Otero, D. Kuang, S. M. Zakeeruddin and M. Grätzel, *J. Phys. Chem. C*, 2007, **111**, 6550–6560.
40 M. Wang, P. Chen, R. Humphry-Baker, S. M. Zakeeruddin and M. Grätzel, *ChemPhysChem*, 2009, **10**, 290–299.
41 J. W. Ondersma and T. W. Hamann, *J. Phys. Chem. C*, 2010, **114**, 638–645.
42 Q. Wang, S. Ito, M. Grätzel, F. Fabregat-Santiago, I. Mora-Sero, J. Bisquert, T. Bessho and H. Imai, *J. Phys. Chem. B*, 2006, **110**, 25210–25221.
43 A. B. F. Martinson, M. S. Goes, F. Fabregat-Santiago, J. Bisquert, M. J. Pellin and J. T. Hupp, *J. Phys. Chem. C*, 2009, **113**, 4015–4021.
44 Q. Wang, Z. Zhang, S. M. Zakeeruddin and M. Grätzel, *J. Phys. Chem. C*, 2008, **112**, 7084–7092.
45 M. K. Nazeeruddin, P. Péchy, T. Renouard, S. M. Zakeeruddin, R. Humphry-Baker, P. Cointe, P. Liska, L. Cevey, E. Costa, V. Shklover, L. Spiccia, G. B. Deacon, C. A. Bignozzi and M. Grätzel, *J. Am. Chem. Soc.*, 2001, **123**, 1613–1624.
46 M. J. Frisch, G. W. Trucks, H. B. Schlegel, G. E. Scuseria, M. A. Robb, J. R. Cheeseman, J. A. Montgomery Jr., T. Vreven, K. N. Kudin, J. C. Burant, J. M. Millam, S. S. Iyengar, J. Tomasi, V. Barone, B. Mennucci, M. Cossi, G. Scalmani, N. Rega, G. A. Petersson, H. Nakatsuji, M. Hada, M. Ehara, K. Toyota, R. Fukuda, J. Hasegawa, M. Ishida, T. Nakajima, Y. Honda, O. Kitao, H. Nakai, M. Klene, X. Li, J. E. Knox, H. P. Hratchian, J. B. Cross, V. Bakken, C. Adamo, J. Jaramillo, R. Gomperts, R. E. Stratmann, O. Yazyev, A. J. Austin, R. Cammi, C. Pomelli, J. Ochterski, P. Y. Ayala, K. Morokuma, G. A. Voth, P. Salvador, J. J. Dannenberg, V. G. Zakrzewski, S. Dapprich, A. D. Daniels, M. C. Strain, O. Farkas, D. K. Malick, A. D. Rabuck, K. Raghavachari, J. B. Foresman, J. V. Ortiz, Q. Cui, A. G. Baboul, S. Clifford, J. Cioslowski, B. B. Stefanov, G. Liu, A. Liashenko, P. Piskorz, I. Komaromi, R. L. Martin, D. J. Fox, T. Keith, M. A. Al-Laham, C. Y. Peng, A. Nanayakkara, M. Challacombe, P. M. W. Gill, B. G. Johnson, W. Chen, M. W. Wong, C. Gonzalez and J. A. Pople, *Gaussian 03*Gaussian, Inc., Wallingford, CT, 2003.
47 P. J. Hay and W. R. Wadt, *J. Chem. Phys.*, 1985, **82**, 270.
48 S. I. Gorelsky, SWizard program, http://www.sg-chem.net/.
49 B. C. O'Regan, J. R. Durrant, P. M. Sommeling and N. J. Bakker, *J. Phys. Chem. C*, 2007, **111**, 14001–14010.

